

# Study of Surface-Enhanced Infrared Spectroscopy

## 1. Dependence of the Enhancement on Thickness of Metal Island Films and Structure of Chemisorbed Molecules

Zhijun Zhang and Toyoko Imae<sup>1</sup>

Research Center for Materials Science, Nagoya University, Chikusa, Nagoya 464-8602, Japan

Received May 22, 2000; accepted September 11, 2000

**The dependence of surface-enhanced infrared absorption (SEIRA) on structure and vibration modes of chemisorbates was studied in a reflection-absorption mode by employing self-assembled monolayers of 4-pyridinethiol and 4-nitrothiophenol formed on Au island films deposited on glass substrates. The present work shows that both the electromagnetic and chemical effects contribute to the total SEIRA enhancement, with the former playing a predominant role. Moreover, the bands due to different vibration modes give rise to distinctly different magnitudes of enhancement, suggesting the presence of a chemical origin in the enhanced IR absorption.** © 2001 Academic Press

**Key Words:** surface-enhanced infrared absorption spectroscopy (SEIRAS); surface plasmon absorption; electromagnetic mechanism; chemical effect; Au island film; self-assembled monolayer (SAM); 4-pyridinethiol; 4-nitrothiophenol.

### INTRODUCTION

In 1980 Harstein and colleagues (1) observed for the first time that infrared absorption of molecules can be enhanced by a factor of up to  $10^3$  when molecules are chemisorbed on Ag and Au surfaces. This phenomenon was later denoted by Osawa and Ikeda (2) as surface-enhanced infrared absorption (SEIRA), by analogy with surface-enhanced Raman scattering (SERS) (3). Following steady yet slow progress in the 1980s, it is currently in a major phase of development and growth, mainly due to a series of fundamental studies undertaken by Osawa (4) and others (5, 6). Of the papers published since the discovery of SEIRA phenomenon, nearly half were published in the past three years (5–15). SEIRA is attracting ever increasing interest from researchers in various areas, especially those in the fields of surfaces and interfaces, trace analysis, electrochemistry, biochemistry, and molecular electronics, etc. (4), for several reasons. SEIRA has advantages over SERS in several aspects, e.g., nondestructivity, and over infrared reflection-absorption (IRAS)

spectroscopy in giving a remarkably higher S/N ratio which is more applicable for time-resolved IR study of surface and interface reactions and dynamic processes. Now it seems generally accepted, on the basis of the theoretical and experimental works mentioned above, that (1) the SEIRA effect stems from both electromagnetic and chemical enhancement, with the former playing a predominant role, analogous to SERS; and (2) the similarity of SEIRA spectra measured in ATR, transmission, and RA modes to IRAS implies that there are surface selection rules working in the SEIRA. A full understanding of the nature and mechanism of the SEIRA, however, is required before it can be widely applied. The concepts of SERS may not always be suitable to describe the nature of SEIRA. Merklin and Griffiths (5a) investigated the effect of surface roughness of metal island films in SEIRA and pointed out that the surface rules of SEIRA proposed by Osawa *et al.* (4) may not necessarily be true in all cases. As for the relative contributions of chemical effect to the overall enhancement in SEIRA, very little is reported (4, 5b, 16), and therefore it is far from unambiguous.

In this and the following paper, we report our investigation on the nature of SEIRA by employing a system of self-assembled monolayers (SAMs) of 4-pyridinethiol and 4-nitrothiophenol on Au island films. Such studies may provide new insight into the origins of the surface IR enhancement, as well as approaches to attaining strong SEIRA enhancement. The reasons for choosing the SAMs of 4-pyridinethiol and 4-nitrothiophenol on Au island are as follows: first, the two aromatic molecules, 4-pyridinethiol (17–19) and 4-nitrothiophenol (20), are known to form ordered monolayer films on Ag or Au surfaces with known orientation, which makes it possible to compare the two molecules to discuss the enhancement mechanisms without considering problems caused by differences in the nature of adsorption, that is, chemisorption or physisorption, as well as in molecular orientations. Second, thermally deposited Au island films show strong SEIRA enhancement comparable with that of the analogous Ag films. Moreover, they are more stable than Ag films. In this paper we discuss how structure and vibration modes of adsorbates affect observed SEIRA. The next paper will focus on large

<sup>1</sup> To whom correspondence should be addressed. Fax: +81-52-789-5912. E-mail: [imaie@chem2.chem.nagoya-u.ac.jp](mailto:imaie@chem2.chem.nagoya-u.ac.jp).

enhanced IR absorption obtained in the transmission mode for the SAM of 4-pyridinethiol sandwiched by Au island films.

## EXPERIMENTAL SECTION

**Chemicals.** 4-Pyridinethiol (95%) and 4-nitrothiophenol were purchased from Aldrich and used without further purification. All other reagents are commercially available and of analytical grade.

**Au island film deposition.** The island films of gold used for the SEIRA experiment were prepared through thermal vapor evaporation onto flat glass substrates in a vacuum chamber at a pressure of about  $10^{-6}$  Torr. The thickness and deposition rate were monitored with a quartz crystal oscillator. The Au deposition rate was maintained at  $0.1 \text{ \AA/s}$  throughout the depositing process. To make a reliable comparison of SEIRA spectra of different SAMs, Au island films with the same thickness used for formation of different SAMs were prepared at the same time. Examination of these films by UV-vis spectral measurement indicated that they were practically identical.

Two-hundred-nanometer Au films evaporated on glass with a 150-nm chromium film as an adhesion layer were used for the IRAS measurement.

**SAM formation.** SAMs were fabricated by soaking freshly prepared Au island films in a  $1 \times 10^{-3}$  M ethanol solution of 4-pyridinethiol or 4-nitrothiophenol for 5 min at room temperature, followed by copious rinsing with ethanol. Care must be taken during the washing and handling processes to avoid peeling off or scratching the island film. Thus-prepared SAM samples were used immediately for spectral measurement.

**UV-vis measurement.** Ultraviolet-visible spectra of Au island films before and after formation of the SAMs of 4-pyridinethiol and 4-nitrothiophenol were recorded on a Shimadzu UV-2200 spectrophotometer. A blank glass substrate was always used as a reference.

**Infrared measurement.** Infrared spectral measurement was taken with a Bio-Rad FTS 575C FT-IR spectrometer equipped with a liquid nitrogen-cooled MCT detector. All spectra were recorded using the coaddition of 1024 scans at  $4 \text{ cm}^{-1}$ . The reflection spectra were measured using a Harrick reflectance attachment with an incidence angle of  $75^\circ$ . The background spectrum of the Au island film was measured as a single beam before the formation of the SAM and was used as the reference.

## RESULTS

### Surface Plasmon Mode

Figure 1 shows UV-vis spectra of Au island films deposited onto glass substrates with film thickness of (a) 5, (b) 10, (c) 15, (d) 20, and (e) 26 nm, respectively. A strong absorption band in the visible and/or visible-near-infrared region is observed for all Au island films. This band is attributed to excitation of surface plasmons in the metal (3, 4). It is well known that surface

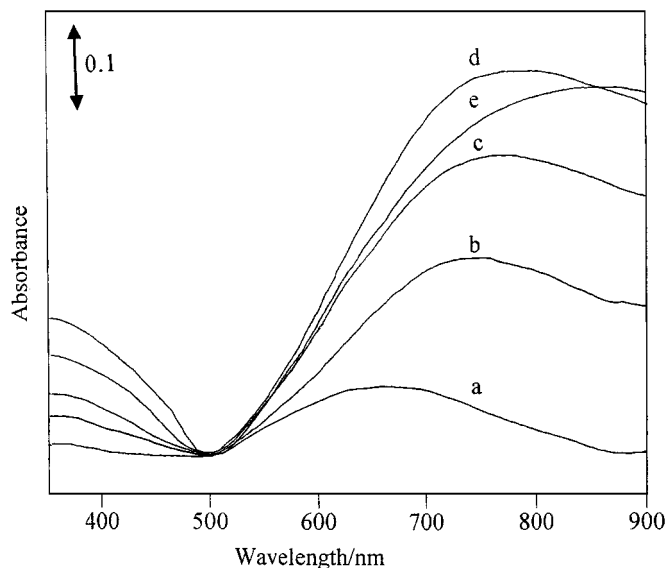


**FIG. 1.** UV-vis spectra of Au island films with thicknesses of (a) 5, (b) 10, (c) 15, (d) 20, and (e) 26 nm.

plasmon modes play an important role in the SEIRA, as in the case of SERS (3, 4). It is clearly seen from Fig. 1 that with the initial increase in the thickness of the Au island film, the surface plasmon band becomes stronger and shifts toward the longer wavelength side. The absorbance seems saturated when the film thickness reaches 20 nm. Above 20 nm thick, the absorbance of the plasmon resonance no longer increases, but the maximum position still shifts toward the near-infrared side. We will correlate it to the observed SEIRA later in this article.

When a SAM is formed at the surface of the metal films, the monolayer film modulates the optical and electromagnetic properties of the Au island film significantly, as evidenced by a significant decrease in absorption, and also somewhat of a shift of the surface plasmon band, depending on the thickness of the Au island films (data not shown). It is clear that the chemical bonding of thiols to the Au atoms at the surface of the island film and the possible etching of the Au surface during SAM formation (21) are responsible for the observed changes in the UV-vis spectra.

### IR Spectra of 4-Pyridinethiol

Figure 2a presents an IRA spectrum of a thick Au substrate after immersion in an ethanol solution of 4-pyridinethiol. For the purpose of comparison, an IR transmission spectrum of 4-pyridinethiol solid dispersed in a KBr pellet is also added as Fig. 2b. IR band assignments were made on the basis of previous literature (7b, 18a, 22, 23), and are listed in Table 1. It is noted that the SAM shows some spectral features rather different from those of the solid state. A band at  $2548 \text{ cm}^{-1}$  due to S-H stretching that appears in the KBr pellet completely disappears in the IRAS spectra, indicating successful formation of a SAM of 4-pyridinethiol on the Au surface. Absorption bands at 1613, 1473, and  $1211 \text{ cm}^{-1}$  due to  $8a$ ,  $19a$  ( $\text{C}=\text{C}$  and  $\text{C}=\text{N}$  stretching

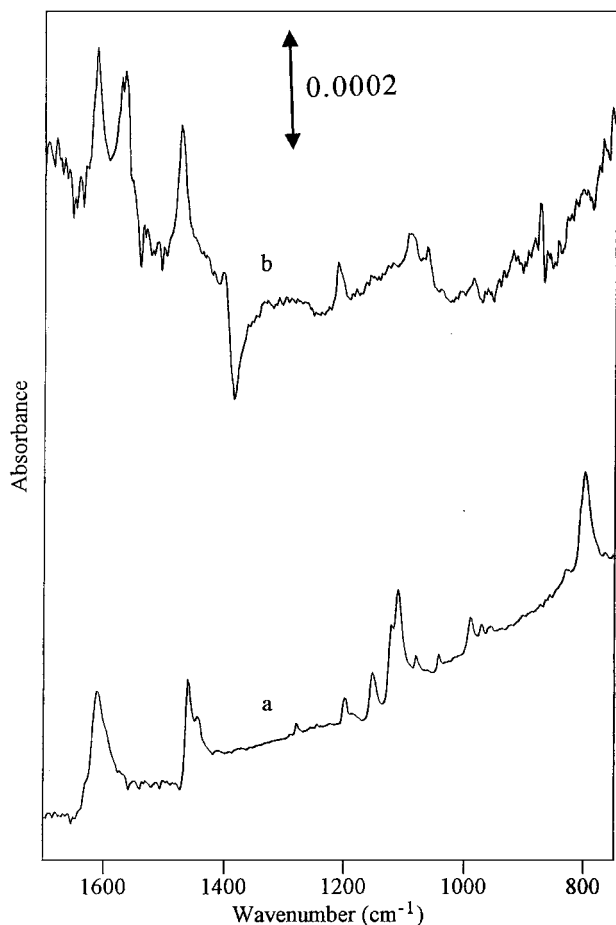


**FIG. 2.** (a) IR transmission spectrum of 4-pyridinethiol dispersed in a KBr pellet (absorbance in au) and (b) IR RA spectrum of a SAM of 4-pyridinethiol on the surface of a thick Au film evaporated on a glass substrate.

modes) and C–H in-plane stretching modes, respectively, appear clearly in the spectrum of the SAM, whereas those due to out-of-plane bending and other modes in the low-wavenumber side are missing or notably weakened, compared with the KBr

**TABLE 1**

**IR Band Frequencies ( $\text{cm}^{-1}$ ) and Assignments for 4-Pyridinethiol**

Band frequencies <sup>a</sup>			
KBr Pellet	IRAS	SEIRA	Assignment <sup>b</sup>
1610 s	1613 s	1612 s	ring str. ip (8a)
	1572 s	1571 s	ring str. ip (8b)
	1565 s	1562 s	
	1473 s	1472 s	ring str. ip (19a)
1460 s		1463 s	
1444 m			ring str. ip (19b)
1198 w	1211 w	1211 w	CH bend ip (3)
1109 s	1093 w		CH bend ip (9a, 15)
988 w	986 w		ring str. ip (1)
789 s			CH bend op ( $2 \times 16a$ )

<sup>a</sup> Relative intensity: s, strong; m, medium; w, weak.

<sup>b</sup> ip, in-plane; op, out-of-plane.

spectrum. The result is, in general, consistent with a previous report by Porter *et al.* (22). The presence of two split bands at 1572 and 1565  $\text{cm}^{-1}$  in the SAM spectrum but not in the KBr, assignable to the ring stretching mode 8b of the pyridine (18a, 23), may not necessarily result from chemisorption as suggested previously (22), since we also observed it in the transmission IR spectrum of 4-pyridinethiol as a film cast on a  $\text{CaF}_2$  substrate (data not shown). The appearance of the bands due to the 8b mode in the SAM and cast film may be related to changes in intermolecular interactions in the film environment compared with those in the KBr pellet. According to the surface selection rule in IRAS, only vibrations with a component perpendicular to the metal surface can interact with the surface electric field that is vertical to the metal surface, and consequently, show IR activity in RAS. The observation of the in-plane ring stretching and C–H deformation modes of the pyridine chemisorbed on the Au surface leads us to a reasonable conclusion that the pyridine plane assumes a nearly vertical orientation to the Au surface, with the  $C_{2v}$  axis through sulfur and nitrogen atoms tilted slightly with respect to the surface normal (17–19).

SEIRA spectra in the 1700 to 1400  $\text{cm}^{-1}$  region of the SAM of 4-pyridinethiol on Au island films with various thickness are shown in Fig. 3. The frequencies of major SEIRA bands are given in Table 1. The profiles of SEIRA spectra resemble those of IRAS, confirming that SEIRA and IRAS share the same surface selection rules (4). It is interesting to note that, compared with the KBr spectrum, the ring stretching bands in the SEIRA, as well as in IRAS, show appreciable shifts.

As shown in Fig. 3, the IR absorption increases monotonically and reaches a maximum with the thickness of the Au island films from 5 to 20 nm, followed by a falloff as the thickness of the Au island film is further increased to 26 nm. For clarity of comparison, we calculated the ratio of band absorbance in SEIRA for Au films of different thicknesses to the corresponding band absorbance in IRAS and listed it in Table 2. We refer to the ratio as *relative enhancement factor* to distinguish it from the term *enhancement factor* that is defined as the absorption intensity ratio with and without a metal film usually used in SEIRA and SERS. A plot of relative enhancement factors for the three bands due to 8a, 8b, and 19a ring stretching modes versus thickness of the Au island films is given in Fig. 4. Correlating the SEIRAS

**TABLE 2**

**Relative Enhancement Factors in RA SEIRA of the SAM of 4-Pyridinethiol on Au Island Films Deposited on Glass Substrates**

Thickness of Au film (nm)	Band frequencies ( $\text{cm}^{-1}$ )		
	1612	1571	1472
5	3	3	2
10	21	33	18
15	43	36	25
20	73	42	44
26	4	4	3

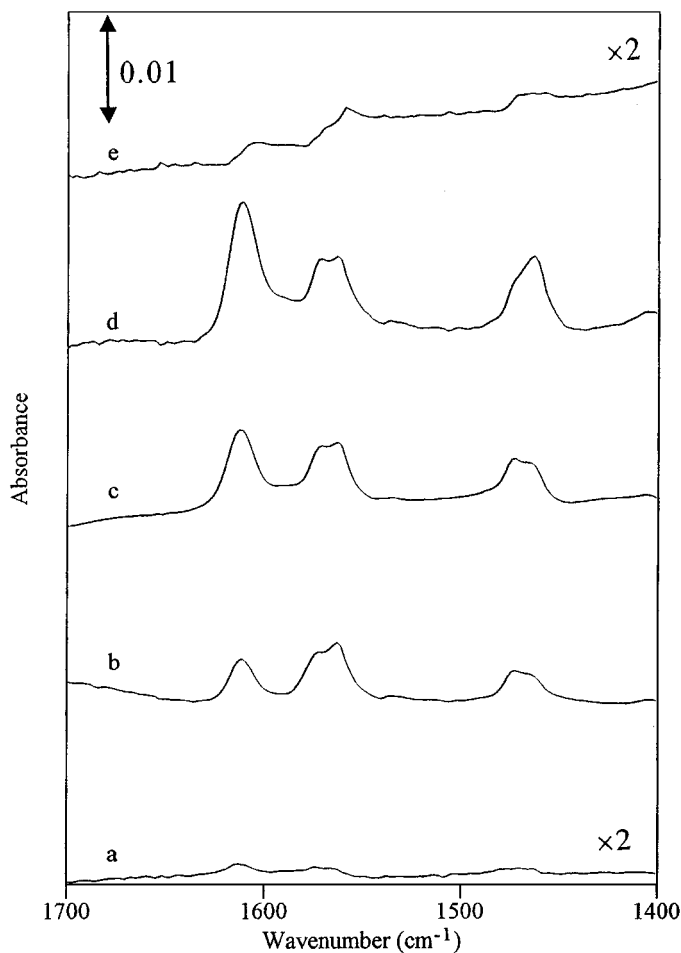


FIG. 3. RA SEIRA spectra of SAMs of 4-pyridinethiol on Au island films with thicknesses of (a) 5, (b) 10, (c) 15, (d) 20, and (e) 26 nm.

to the surface plasmon bands in the UV-vis spectra of Au island films with different thickness (5, 10, 15, 20, and 26 nm) (Fig. 1) suggests a predominant contribution of the electromagnetic mechanism, similar to previous studies by others on SEIRA (4).

#### IR Spectra of 4-Nitrothiophenol

Like 4-pyridinethiol, 4-nitrothiophenol forms SAMs easily on the Au surface. The IRAS of the SAM of 4-nitrothiophenol on a thick Au surface, as well as the transmission spectrum of the 4-nitrothiophenol in a KBr pellet, is shown in Fig. 5. The band assignment is made according to previous work (24) and is tabulated in Table 3. Apparently, the bands attributed to  $a_1$  modes (in  $C_{2v}$  symmetry) of the phenyl group as well as those at 1346 and 855  $\text{cm}^{-1}$  due to symmetric stretching and scissoring modes of the nitro group give a strong absorption in the IRAS, similarly to that observed by Osawa (4). The band at 1522  $\text{cm}^{-1}$  ascribed to the antisymmetric stretching mode of the nitro group has absorbance comparable to that of its symmetric one in the KBr pellet, but it becomes considerably weak compared to its symmetric mode in IRAS. In addition, a strong band at 837  $\text{cm}^{-1}$

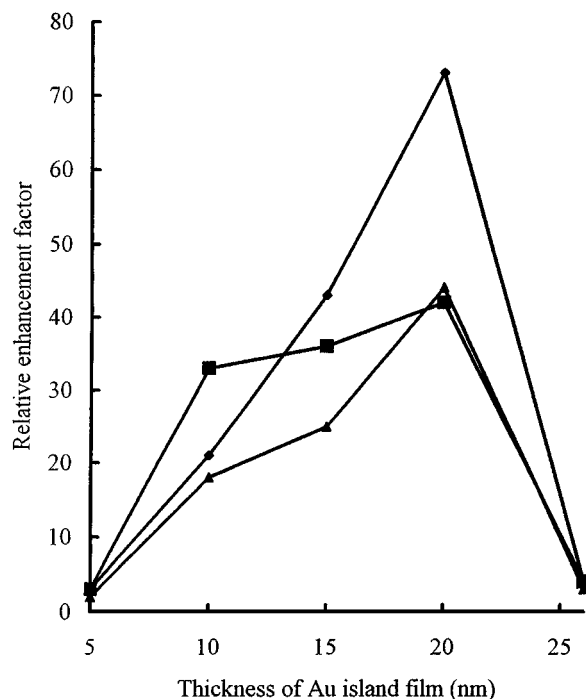


FIG. 4. Plot of the relative enhancement factors for the bands at 1612 (◆), 1571 (■), and 1472 (▲)  $\text{cm}^{-1}$  due to 8a, 8b, and 19a modes of the pyridine group, respectively, in SEIRA spectra of the SAMs of 4-pyridinethiol as a function of the thickness of the Au island film.

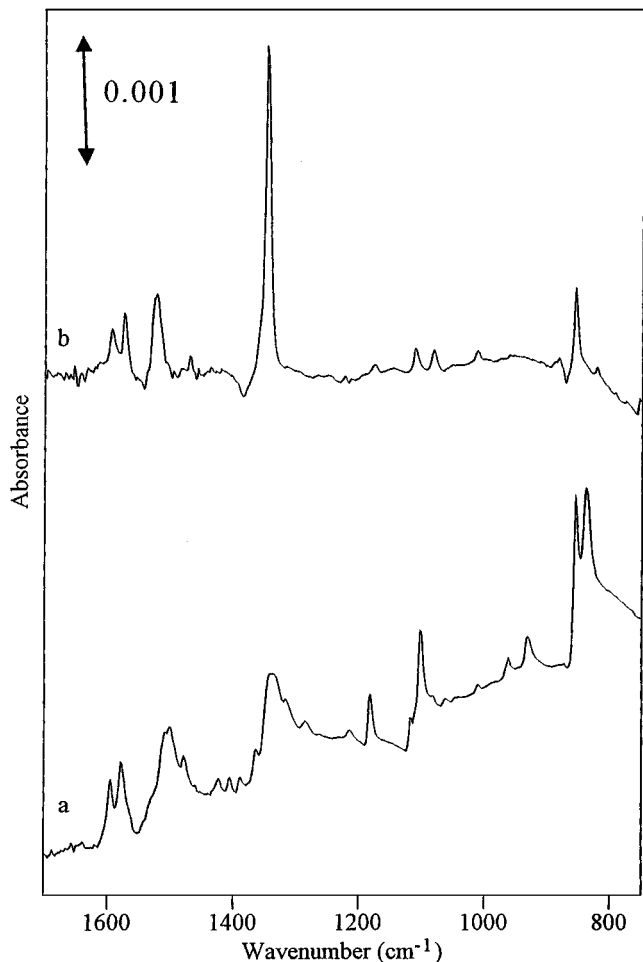
assignable to out-of-plane bending of the ring which is as strong as the band located at 854  $\text{cm}^{-1}$  in the KBr matrix is missing in the IRAS. This observation strongly suggests that the phenyl plane is oriented vertical to the Au surface with the  $C_{2v}$  axis perpendicular to the surface.

TABLE 3  
IR Band Frequencies ( $\text{cm}^{-1}$ ) and Assignment  
for 4-Nitrothiophenol

Band frequencies <sup>a</sup>			
KBr pellet	IRAS	SEIRA	Assignment <sup>b</sup>
3097 w	3082 w	3085 w	CH str. ip (2)
2548 w			SH str.
1594 s	1594 m	1593 w	ring str. ip (8a)
1577 s	1573 m	1571 m	ring str. ip (8b)
1507 s	1522 m	1512 m	NO <sub>2</sub> asym str.
1477 m	1469 w	1469 w	ring str. ip (19a)
1336 s	1346 vs	1336 vs	NO <sub>2</sub> sym str.
1181 m	1175 w	1174 w	ring str. ip (9a)
1100 s	1110 w	1108 w	CH bend ip (15)
1078 w	1081 w	1077 w	CS str. ip (7a)
1008 w	1011 w	1009 w	CC bend ip (18a)
854 vs	855 s	853 s	NO <sub>2</sub> bend ip
837 vs			CH bend op (10a)

<sup>a</sup> Relative intensity: vs, very strong; s, strong; m, medium; w, weak.

<sup>b</sup> ip, in-plane; op, out-of-plane.



**FIG. 5.** (a) IR transmission spectrum of 4-nitrothiophenol dispersed in a KBr pellet (absorbance in au) and (b) IR RA spectrum of a SAM of 4-nitrothiophenol on the surface of a thick Au film evaporated on a glass substrate.

The SEIRA spectra show profiles similar to those of the IRAS, as are seen in spectra a to e of Fig. 6. The relative enhancement factors for various bands in SEIRA are calculated and listed in Table 4. To facilitate discussion later, we plot the three ring stretching modes and three NO<sub>2</sub> vibration modes against the thickness of Au island films (Figs. 7 and 8). Like

**TABLE 4**

**Relative Enhancement Factors in RA SEIRA of the SAM of 4-Nitrothiophenol on Au Island Films Deposited on Glass Substrates<sup>a</sup>**

Thickness of Au film (nm)	Band frequencies (cm <sup>-1</sup> )									
	1593	1571	1512	1469	1336	1174	1108	1077	1009	853
5	2	9	5	5	6	8	6	12	6	6
10	8	19	13	16	12	15	10	21	16	14
15	21	60	32	43	33	54	32	47	55	39
20	30	71	47	59	43	79	44	40	N	77
26	2	3	N	3	5	3	2	N	N	2

<sup>a</sup> N refers to those difficult to determine due to spectral distortion.

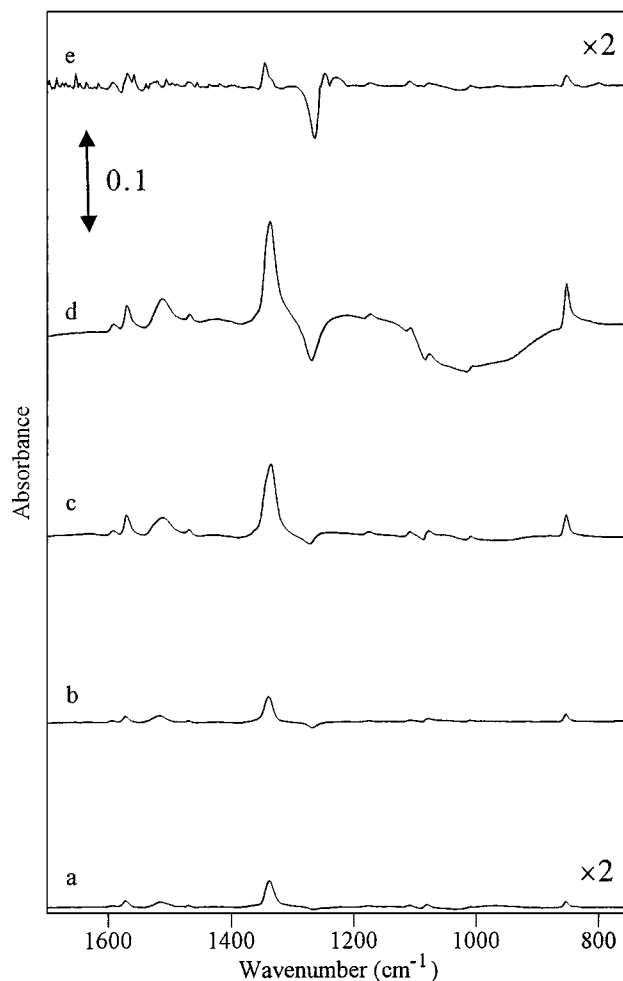


**FIG. 6.** RA SEIRA spectra of SAMs of 4-nitrothiophenol on Au island films with thicknesses of (a) 5, (b) 10, (c) 15, (d) 20, and (e) 26 nm.

4-pyridinethiol, clearly, all IR bands were enhanced with the increase of Au film thickness. The absorption reaches a maximum at the film thickness of 20 nm and then decreases steeply. It is noteworthy that the largest relative enhancement factors of more than 70 are observed for a band at 1571 cm<sup>-1</sup> due to stretching mode 8b of the phenyl ring, and a band at 853 cm<sup>-1</sup> due to in-plane bend of the nitro group. We will discuss this further in the Discussion section.

## DISCUSSION

### *Electromagnetic Mechanism*

Correlating the SEIRA spectra to the surface plasmon bands in the UV-vis spectra enables us to explore the mechanisms of the enhancement. Both the absorbance of the plasmon band in the UV-vis spectra and the relative enhancement factor of various bands in SEIRA for the SAMs of 4-pyridinethiol and 4-nitrothiophenol show a steady increase with the thickness of the Au film up to 20 nm. However, when the thickness of the

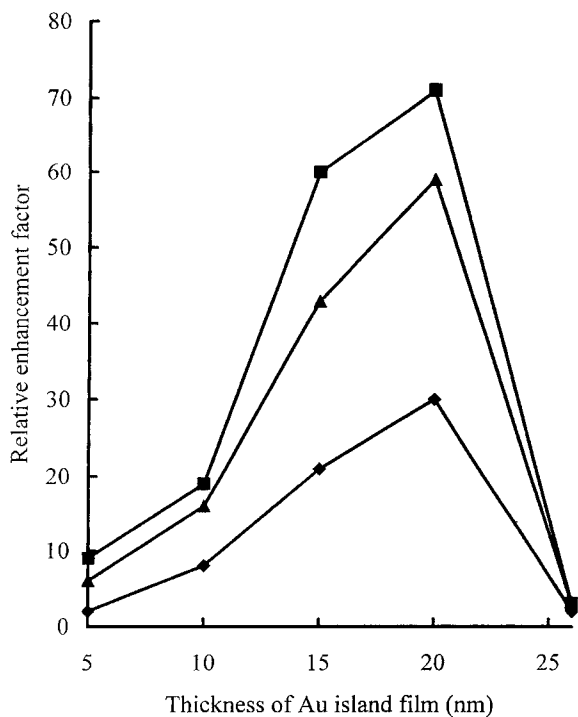


**FIG. 7.** Plot of the relative enhancement factors of bands at 1593 (◆), 1571 (■), and 1469 (▲)  $\text{cm}^{-1}$  due to 8a, 8b, and 19a ring stretching modes of the phenyl group, respectively, in SEIRA spectra of the SAMs of 4-nitrothiophenol as a function of the thickness of the Au island film.

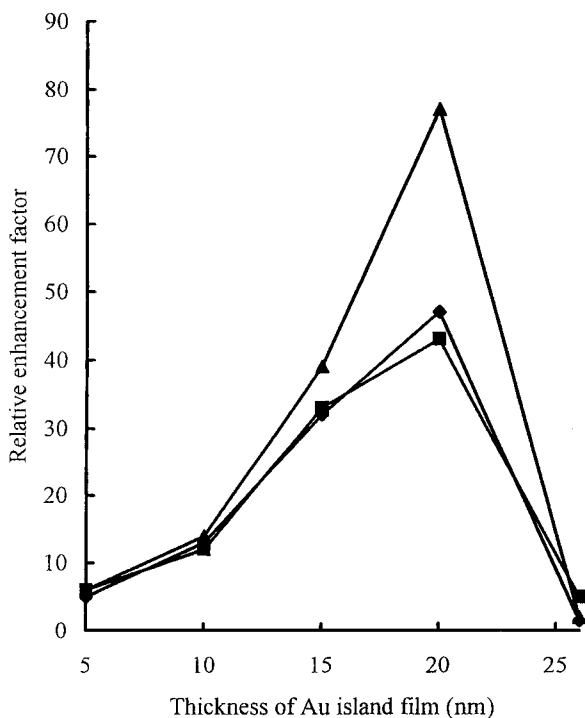


**FIG. 8.** Plot of the relative enhancement factors for the three bands at 1512 (◆), 1336 (■), and 853 (▲)  $\text{cm}^{-1}$  due to antisymmetric stretching, symmetric stretching, and bending modes, respectively, of the nitro group in SEIRA spectra of the SAMs of 4-nitrothiophenol as a function of the thickness of the Au island film.

film reaches 26 nm, the absorbance of the surface plasmon band was saturated, whereas the relative enhancement factors for all vibrational bands in the SEIRA for both molecules drop steeply. The results indicate strongly the dependence of the SEIRA effect on surface plasmon absorption modulated by the thickness of the Au films. At a thickness of 26 nm, the Au island film shows a continuous structure, and, therefore, becomes a poor SERS (25, 26) and SEIRA (27) enhancer. We mentioned that the two molecules show nearly the same tendency in SEIRA with the thickness of the island films. Plots of the relative enhancement factor for both molecules versus the thickness of the Au island films in Figs. 4 and 7 provide us important information on enhancement mechanisms in the present experiment. The Au films used for formation of SAMs of the two molecules were prepared at the same time, and UV examination shows the films are practically identical. Moreover, as discussed in the last section, the two molecules chemisorbed on the Au surface with approximately the same orientation. Therefore, we assume the two adsorbates interacted with electric fields of comparable amplitude. Consequently, they are expected to have similar enhancement tendencies. We observed such a pattern in Figs. 4, 7, and 8, irrespective of the chemical structure of the molecules and of different vibration modes in the same molecules. Thus, we conclude that the electromagnetic effect plays a predominant role in the overall enhancement.

#### Chemical Effect

It is clear that the electromagnetic mechanism plays a predominant role in the observed SEIRA, as evidenced by the plots for the ring stretching and  $\text{NO}_2$  modes in Figs. 4, 7, and 8. It is, however, interesting to note that two molecules as well as the bands due to different vibration modes in the same molecule give different enhancements. An electromagnetic mechanism cannot explain why some bands are enhanced more, while others are enhanced less. These facts suggest involvement of additional origins in the surface-enhanced vibration spectroscopies. In a review on the mechanisms of SERS, Otto *et al.* (3(b)) proposed a model of adsorbates on a metal surface that can account for the chemical specificity and vibrational selectivity of SERS. In an investigation of ATR SEIRA of *p*-nitrobenzoic acid (PNBA) with Ag films, Badilescu and his colleagues (16) observed that the much stronger enhancements were from those groups that were strongly polarizable, like  $\text{COOH}$  and  $\text{NO}_2$ , while those of C–H stretching and bending modes give relatively smaller enhancement. They inferred that the polar groups usually show a large change in dipole moment during vibration and thus give a strong IR enhancement. Merklin and Griffiths (5) further explained it as a donor–acceptor interaction with the metal surface. Our experimental results, however, are not in complete agreement with their observations and conclusions.

Taking SEIRAS of the SAM of 4-nitrothiophenol as an example, the bands at 3085 and 1108  $\text{cm}^{-1}$  assignable to a C–H stretching mode and a C–H in-plane bending mode, respectively, do exhibit rather weak enhancement (relative enhancement

factor less than 20 in the case of 20-nm Au island film). Surprisingly yet interestingly, the band due to the *8b* mode of the phenyl group gives a stronger enhancement (relative enhancement factor of 71) than both bands due to symmetric and antisymmetric stretching modes of NO<sub>2</sub> (relative enhancement factor of 43 and 47, respectively), which is a more strongly polarizable group than C=C of phenyl group. This cannot be an artifact because we also observed a similar phenomenon in the case of 10- and 15-nm Au island films, respectively (see Table 4). This observation is apparently in contradiction with the explanation proposed by Badilescu and his colleagues (16).

Moreover, by examining various vibration modes of the nitro group, we found that the largest enhancement is observed not for the bands at 1336 or 1512 cm<sup>-1</sup> due to the symmetric or the antisymmetric stretching modes, but is observed for that due to the in-plane bending mode. It was originally expected that the band at 1336 cm<sup>-1</sup> should give the largest enhancement (5b, 19), because the gradient of the dipole moment of NO<sub>2</sub> is larger during a stretching movement than during a bending one. It is difficult to give a definite interpretation of our observations at present, but it is likely that vibronic coupling of vibration modes with the charge transfer between the chemisorbed pyridine or the phenyl group and the Au surface is related to the experimental results. Further work to elucidate such a phenomenon is presently underway in this laboratory.

The enhancements of bands due to the same ring stretching modes for 4-pyridinethiol and 4-nitrothiophenol were originally expected to be significantly different from each other, since the chemical effect, i.e., the charge transfer of the Au surface with 4-pyridinethiolate seems to be significantly different from that with 4-nitrothiophenolate. The presence of a NO<sub>2</sub> group in the 4-nitrothiophenol should promote the donor-acceptor interaction described by Merklin and Griffiths (5b). We observed that for the bands (at 1612 cm<sup>-1</sup> for 4-pyridinethiol and at 1593 cm<sup>-1</sup> for 4-nitrothiophenol) due to the *8a* mode, the pyridine shows enhancement roughly 2 times larger than that of 4-nitrothiophenol. In contrast, in the case of *8b*, 4-nitrothiophenol gives an enhancement considerably larger than that of 4-pyridinethiol. As for the *19a* mode, the two molecules show no noticeable difference. Elucidation of these data needs further theoretical and experimental efforts. One thing that should be kept in mind when one analyzes these data is that the molecules may exist in different states in the SAM. Taking the SAM of 4-pyridinethiol on coinage metal surfaces as an example, the N atom of the pyridyl group in the SAM may have a positive charge in certain cases that were reported previously (28). If this is the case, the positively charged pyridine SAM should interact with the Au film, and thus yield a SEIRA effect different from that of the neutral one, as may be expected.

## CONCLUSION

To summarize, a study on the nature of SEIRA by employing an Au island film-SAM system was presented. The

present work suggests that electromagnetic and chemical mechanisms are operating in the observed SEIRA, with the former playing a dominant role in enhancement of the IR absorption.

## ACKNOWLEDGMENTS

Z.Z. gratefully acknowledges the Japan Society for the Promotion of Science (JSPS) for a postdoctoral fellowship for foreign researchers.

## REFERENCES

1. Harstein, A., Kirtley, J. R., and Tsang, J. C., *Phys. Rev. Lett.* **45**, 201 (1980).
2. Osawa, M., and Ikeda, M., *J. Phys. Chem.* **95**, 9914 (1991).
3. (a) Chang, K., Furtak, T. E., "Surface Enhanced Raman Scattering," Plenum Press, New York, 1982; (b) Otto, A., Mrozek, I., Grabhorn, H., and Akemann, W., *J. Phys. Condens. Matter* **4**, 1143 (1992).
4. (a) Suétaka, W., "Surface Infrared and Raman Spectroscopy: Methods and Application," Plenum Press, New York, 1995; (b) Osawa, M., *Bull. Chem. Soc. Jpn.* **70**, 2861 (1997), and references cited therein.
5. (a) Merklin, G. T., and Griffiths, P. R., *J. Phys. Chem. B* **101**, 5810 (1997); (b) Merklin, G. T., and Griffiths, P. R., *Langmuir* **13**, 6159 (1997); (c) Bjerke, A. E., Griffiths, P. R., and Theiss, W., *Anal. Chem.* **71**, 1967 (1999).
6. (a) Aroca, R., and Price, B., *J. Phys. Chem. B* **101**, 6537 (1997); (b) Aroca, R., and Bujalski, R., *Vib. Spectrosc.* **19**, 11 (1999).
7. (a) Osawa, M., and Yoshii, K., *Appl. Spectrosc.* **51**, 512 (1997); (b) Cai, W., Wan, L., Noda, H., Hibino, Y., Ataka, K., and Osawa, M., *Langmuir* **14**, 6992 (1998); (c) Ataka, K., and Osawa, M., *Langmuir* **14**, 951 (1998); (d) Sato, S., Kamada, K., and Osawa, M., *Chem. Lett.* **15** (1999); (e) Sun, S., Cai, W., Wan, L., and Osawa, M., *J. Phys. Chem. B* **103**, 2460 (1999); (f) Noda, H., Ataka, K., Wan, L., and Osawa, M., *Surf. Sci.* **427-428**, 190 (1999).
8. Kang, S. Y., Jeon, I. C., and Kim, K., *Appl. Spectrosc.* **52**, 278 (1997).
9. (a) Zhao, J., Zhang, J., He, H. X., Li, H. L., and Liu, Z. F., *Chem. Phys. Lett.* **278**, 220 (1997); (b) Zhang, J., Zhao, J., He, H. X., Zhang, H. L., Li, H. L., and Liu, Z. F., *Langmuir* **14**, 5521 (1998).
10. (a) Brown, C. W., Li, Y., Seelenbinder, J. A., Pivarnik, P., Rand, A. G., Letcher, S. V., Gregory, O. J., and Platek, M., *Anal. Chem.* **70**, 2991 (1998); (b) Seelenbinder, J. A., Brown, C. W., Pivarnik, P., and Rand, A. G., *Anal. Chem.* **71**, 1963 (1999).
11. Wanzenbock, H. D., Mizaiakoff, B., Weissenbacher, N., and Kellner, R., *Fresenius J. Anal. Chem.* **362**, 15 (1998).
12. Suzuki, Y., Seki, H., Inamura, T., Tanabe, T., Wadayama, T., and Hatta, A., *Surf. Sci.* **427-428**, 136 (1999).
13. Maroun, F., Ozanam, F., Chazalviel, J.-N., and Theiß, W., *Vib. Spectrosc.* **19**, 193 (1999).
14. Han, H. S., Han, S. W., Joo, S. W., and Kim, K., *Langmuir* **15**, 6868 (1999).
15. Jensen, T. R., Van Duyne, R. P., Johnson, S. A., and Maroni, V. A., *Appl. Spectrosc.* **54**, 371 (2000).
16. (a) Badilescu, S., Ashrit, P. V., and Truong, V. V., *Appl. Phys. Lett.* **52**, 1551 (1988); (b) Badilescu, S., Ashrit, P. V., Truong, V. V., and Badilescu, I. I., *Appl. Spectrosc.* **43**, 549 (1989).
17. (a) Gui, J. Y., Lu, F., Stern, D. A., and Hubbard, A. T., *J. Electroanal. Chem.* **292**, 245 (1990); (b) Zhang, Z.-J., Hou, S. F., Zhu, Z. H., and Liu, Z. F., *Langmuir* **16**, 537 (2000).
18. (a) Christensen, P. A., Hammett, A., and Blackman, I., *J. Electroanal. Chem.* **318**, 407 (1991); (b) Taniguchi, I., Yoshimoto, S., and Nishiyama, K., *Chem. Lett.* **353** (1997).

19. Sawaguchi, T., Mizutani, F., and Taniguchi, I., *Langmuir* **14**, 3565 (1998).
20. Matsuda, N., Yoshii, K., Ataka, K., Osawa, M., Matsue, T., and Uchida, I., *Chem. Lett.* 1385 (1992).
21. Schönenberger, C., Sondag-Huethorst, J. A. M., Jorritsma, J., and Fokkink, L. G. J., *Langmuir* **10**, 611 (1994), and references cited therein.
22. Lamp, B. D., Hobara, D., Porter, M. D., Niki, K., and Cotton, T. M., *Langmuir* **13**, 736 (1997).
23. Kline, Jr., C. H., and Turkevich, J., *J. Chem. Phys.* **12**, 300 (1944).
24. Colthup, N. B., Daly, L. H., and Wiberley, S. E., "Introduction to Infrared and Raman Spectroscopy," 3rd Ed., Academic Press, San Diego, 1990.
25. Schlegel, V. L., and Cotton, T. M., *Anal. Chem.* **63**, 241 (1991).
26. Van Duyne, R. P., Hulteen, J. C., and Treichel, D. A., *J. Chem. Phys.* **99**, 2101 (1993).
27. Nishikawa, Y., Nagasawa, T., Fujiwara, K., and Osawa, M., *Vib. Spectrosc.* **6**, 43 (1993).
28. (a) Bryant, M. A., and Crooks, R., *Langmuir* **9**, 385 (1993); (b) Yu, H. Z., Xia, N., and Liu, Z. F., *Anal. Chem.* **71**, 1354 (1999).